Theoretical investigation of the alkaline-earth dihydrides from relativistic all-electron, pseudopotential, and density-functional study

Ivan S. Lim and Yoon Sup Lee[a)]
Quantum and Computational Chemistry Laboratory, Department of Chemistry, School of Molecular Science (BK21), KAIST, 373-1 Guseong-dong, Yuseong-gu, Daejoen 305-701, Korea

(Received 15 November 2006; accepted 4 January 2007; published online 14 March 2007)

Highly precise ground state geometries, harmonic vibrational frequencies and force constants of alkaline-earth dihydrides from CaH_2 to RaH_2 are obtained using relativistic small-core energy-consistent effective core potentials at the coupled-cluster level. The results are compared with all-electron as well as density functional calculations. All-electron results, in particular, clearly show the importance of relativistic effects in the properties considered in this paper. The monotonic trends in the geometries are explained in terms of second-order perturbation theory. Trends in the force constants are monotonic except for the bending mode where an anomaly occurs from BaH_2 to RaH_2. It is rationalized in terms of reduced *s-d* hybridization due to relativity, which is shown to be an energy effect attributed to the stabilization of the *s* orbital. The pseudopotentials show an excellent performance in comparison with all-electron methods and are therefore successfully transferred to molecular cases. The density functional methods, however, suffer from functional dependencies with B3LYP performing the best in this case. © *2007 American Institute of Physics*. [DOI: 10.1063/1.2437213]

I. INTRODUCTION

The peculiar geometry of the triatomic molecules of AB_2 involving alkaline-earth metals and either hydrogen or halides has been a long-standing problem in inorganic chemistry for many years.[1] Since the first experimental observation[2] of permanent electric-dipole moments, there have been various attempts to offer explanations and predictions for the question of bending in these molecules. Such investigations resulted in many research papers and review articles. In one of the first papers offering a rationalization for bending, Hayes argued that the participation of the metal *d* orbitals is important and suggested to modify the Walsh diagram to include the contributions from these *d* orbitals for the prediction of the bent structure.[3] It was also shown, through Laplacian of calculated electronic density, that the outer shell of the metal core $[(n-1)d]$ exhibits localized concentration of electronic charge.[4] Guido and Gigli, on the other hand, thought that the core polarization of the metal cation was the main contributing factor for bending and employed the polarized-ion model to calculate the equilibrium configuration of some of AB_2 molecules.[5] More than a decade later, Szentpály and Schwerdtfeger argued that the cation polarizability was not large enough to explain bending, and in fact the two factors could not be taken separately. Consequently, they proposed the use of atomic softness in an attempt to justify and predict linear versus bent structures.[6] This showed, however, some limitations as discussed by Kaupp *et al.* who compared the relative importance of the core polarization versus *d*-orbital participation.[1] They concluded that both factors are important. More recently, Donald *et al.*[7] extended their version of the polarized-ion model based on the Rittner-type electrostatic model to the group 12 metals and found the failure of the model for the group 12 case. Today, the key aspects of bending are well accepted although it is still difficult to uniquely devise a model accurate on a quantitative level. We also note a review article of Kaupp which offers a general discussion extending to systems with a formal d^0 electronic configuration.[8]

Most of recent theoretical studies were performed based on the frozen-core approximation employing relativistic pseudopotentials. Consequently, there are only few papers discussing relativistic effects on these molecules due to the lack of reliable nonrelativistic data. An early study by Pyykkö using relativistic and nonrelativistic Hartree-Fock one-center expansion offered clear evidence for *d*-orbital involvement which is influenced by relativity. Relativistic effects on the bond lengths and vibrational frequencies were, however, reported to be very small for the alkaline-earth dihalides up to Ba through *ab initio* model potential studies.[9] They were found to be more important for the linearization energy for the bent structure.

In this paper we attempt not to revisit the models put forward for the explanation of bending but to rationalize, using these models, the role played by relativity on the general trends in the molecular geometry and harmonic vibration frequencies. In this note we performed all-electron nonrelativistic and scalar relativistic Douglas-Kroll calculations for the equilibrium geometry and the harmonic vibrational frequencies of alkaline-earth dihydrides from CaH_2 to RaH_2. Pseudopotential calculations are also carried out, which is the first application of the relativistic small-core energy-consistent effective core potentials (ECPs) developed recently by the present author. This will test the performance

[a)]Electronic mail: yoonsuplee@kaist.ac.kr

TABLE I. Optimized equilibrium geometries of the alkaline-earth dihydrides, MH_2 (M=Ca to Ra) at various levels of theory. Bond lengths are in angstroms and bond angles are in degrees.

	AE						ECP			
r (M–H)	NRHF	NRMP2	NRCCSD(T)	DKHF	DKMP2	DKCCSD(T)	HF	MP2	CCSD(T)	ECP B3LYP
CaH_2	2.089	2.050	2.061	2.087	2.048	2.060	2.083	2.049	2.060	2.052
SrH_2	2.235	2.171	2.185	2.231	2.168	2.184	2.232	2.169	2.183	2.165
BaH_2	2.349	2.270	2.285	2.356	2.277	2.293	2.356	2.279	2.292	2.288
RaH_2	2.412	2.333	2.346	2.430	2.345	2.365	2.435	2.357	2.372	2.374
$\angle$ (H–M–H)										
CaH_2	180.0	180.0	180.0	180.0	180.0	180.0	180.0	180.0	180.0	180.0
SrH_2	143.4	133.7	134.1	144.1	134.1	134.6	144.8	134.5	134.9	124.6
BaH_2	123.3	118.0	117.9	123.8	117.5	117.3	123.9	117.4	117.3	113.6
RaH_2	120.7	116.3	116.3	119.1	111.4	111.7	119.7	112.7	112.6	109.5

of the pseudopotentials which have been proven successful in atomic cases. Also presented are density functional theory (DFT) results.

II. METHOD

The minimum energy geometries of the alkaline-earth dihydrides were obtained by the use of small-core $(10\nu e)$ scalar relativistic (ARPP) energy-consistent ECPs described in Ref. 10. These ECPs have been successfully tested for the dipole polarizabilities and ionization potentials of neutral and charged atomic species and are particularly suitable for the present case where core-polarization effects are expected to play an important role. The basis sets accompanying the ECPs were used without modification although the effects of additional hard d functions important for the prediction of the bent structure were checked.[11] It turned out that the original basis sets are sufficient in describing the bent structure as additional d exponents did not affect the geometry at all. Valence correlation was treated for all 12 electrons in MH_2 at the second-order Møller-Plesset (MP2) and coupled-cluster singles, doubles, and iterative triples [CCSD(T)] level.

The accuracy of the pseudopotential results were tested against all-electron (AE) calculations performed at the scalar relativistic level employing second-order Douglas-Kroll (DK) Hamiltonian. Nonrelativistic AE calculations were also carried out for the discussion of relativistic effects. The basis sets for the nonrelativistic case were obtained from ANO-RCC basis sets of Roos *et al.*,[12] which were completely decontracted and recontracted with contraction coefficients evaluated in nonrelativistic self-consistent-field calculations. Electron correlation at the AE level was treated at the MP2 and CCSD(T) level. While all electrons were explicitly correlated at the MP2 level, some core shells were left out of correlation at the CCSD(T) level as follows: no frozen core for Ca, frozen KL core for Sr and Ba, and frozen KLM core for Ra. Calculations were performed with GAUSSIAN03,[13] MOLPRO,[14] and MOLCAS[15] program packages.

III. RESULTS AND DISCUSSION

The equilibrium geometry of the alkaline-earth dihydrides obtained at various levels of theory are presented in Table I. One of the key features of the equilibrium geometry is the linear versus bent structure. CaH_2 adopts a linear structure at equilibrium while a progressively more bent structure is favored as the nuclear charge increases. The involvement of the $(n-1)d$ orbital in the bent structure is depicted in Fig. 1 in terms of molecular orbitals (MOs). Clearly, the second highest occupied molecular orbital (HOMO-1) of a_1 symmetry (σ_g for the linear case) shows a metal d_{z^2} character in both the linear and bent structures. Equally evident for the bent structure is the involvement of the metal d_{yz} function in the HOMO of b_2 symmetry. The HOMO of the linear structure is solely given by the σ overlap involving the metal p_z orbital. The monotonic decrease in the bond angle from SrH_2 to RaH_2 may be expected from the second-order perturbation theory.[16] That is, the stabilization upon bending is given by the second-order term of the perturbation energy expression and is inversely proportional to the HOMO-lowest occupied molecular orbital (LUMO) gap of the linear structure. This inverse proportionality then ensures an increase in the degree of stabilization upon bending as the HOMO-LUMO energy gap decreases from SrH_2 to RaH_2 (0.2922, 0.2639, and 0.2543 a.u. for SrH_2 to RaH_2, respectively). This, in turn, gives rise to a monotonically decreasing bond angle with increasing nuclear charge of the metal. There is also a monotonic trend in the M–H bond distance, which is increasing down the group. This trend has been known[11] up to BaH_2 and is found to continue to RaH_2. Clearly, any relativistic effects expected for Ra is not substantial enough to affect the overall trend in the bond lengths, but relativistic contribution, nevertheless, reveals an interesting aspect. This is depicted in terms of the difference in the bond lengths obtained at the Douglas-Kroll Hartree-Fock (DKHF) and nonrelativistic Hartree-Fock (NRHF) levels of theory in Fig. 2. The bond lengths for CaH_2 and SrH_2 are contracted, whereas those for the heavier BaH_2 and RaH_2 are expanded by relativity. It has been argued that these bond contraction and expansion are first-order effects quite unrelated to the orbital contraction and expansion of s and p orbitals and d orbital, respectively.[17] It is clearly shown in this case that the usual bond contraction is completely canceled out as the d orbital becomes more important for the heavier metal dihydrides. For the linear configuration, we find a progressively larger

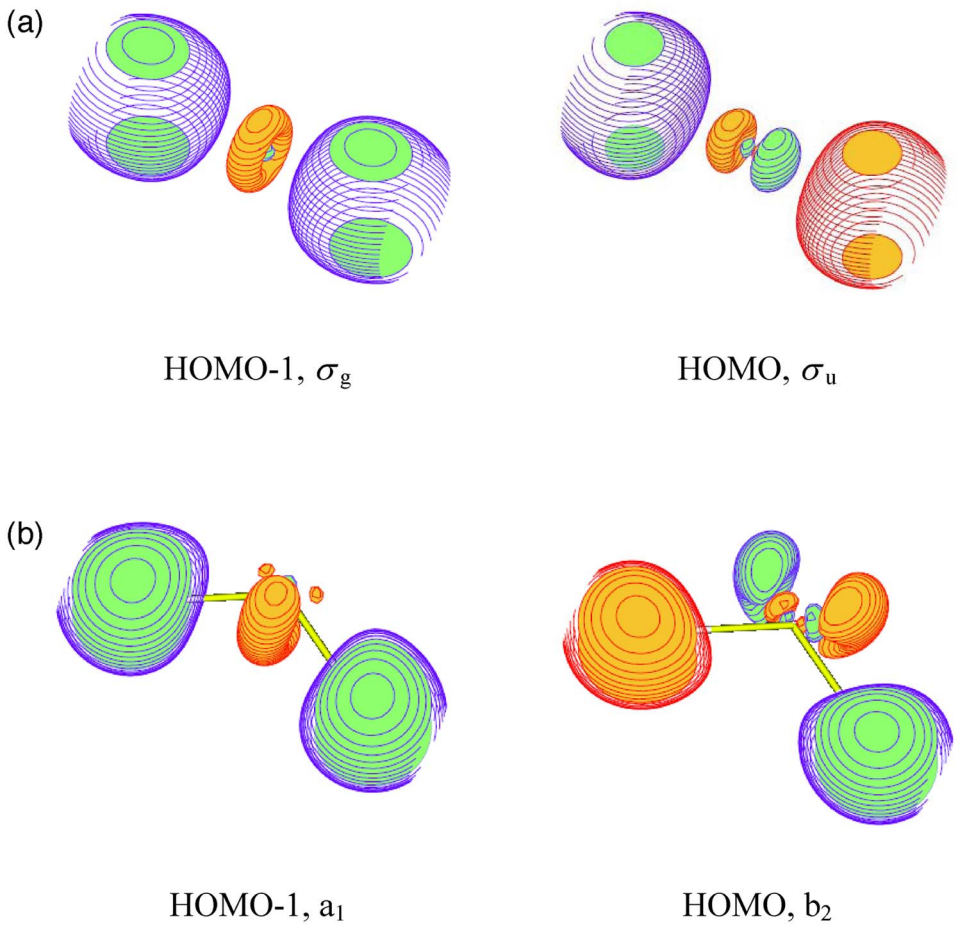

FIG. 1. (Color online) Molecular orbital diagrams of the HOMO and HOMO-1 of (a) CaH_2 and (b) RaH_2 obtained at the nonrelativistic HF level. For the linear CaH_2, the molecule lies in the z axis. For the bent RaH_2, the twofold C_2 axis is defined as the z axis and the yz plane lines on the plane of the paper.

bond length contraction due to relativity with increasing nuclear charge of the metal. In order to test for spin-orbit effects on the bond lengths, we carried out a DFT calculation with two-component spin-orbit pseudopotential and B3LYP functional for RaH_2. It is found that there is a little bond length contraction of 0.03 Å due to spin-orbit effects and negligible contribution to the bond angle.

As for electron correlation effects, there are no big surprises. The contribution is indicating that the Hartree-Fock (HF) bond lengths are too long and bond angles too large. Referring to the nonrelativistic results at the CCSD(T) level (Table I), the reduction in the bond length grows with the nuclear charge of the metal to a maximum of 0.07 Å for RaH_2. The bond angle, however, shows an opposite trend in which correlation effects diminish down the group with the largest contribution of 9.3° for SrH_2. In order to explain this trend we consider the factors important for bending, one of which is the dipole polarizability of the metal cation. It turns out that the metal cations become less polarizable at the correlated level.[18] The amount of depolarization grows with increasing nuclear charge, which then gives rise to an increasing tendency to oppose bending from CaH_2 to RaH_2. This tendency to linearize on electron correlation from the viewpoint of dipole polarizability then counterbalances the overall effects of electron correlation which make the molecules more bent. Unusually large correlation effects observed for RaH_2 at the DKCCSD(T) level can be related to the dipole polarizabilities as well since the correlation contribution to the dipole polarizability of Ra^{2+} becomes slightly positive at the DKCCSD(T) level. As a result, the bending tendency increases upon correlation and there arises an anomalous trend in the correlation contribution to the bond angle at the relativistic level.

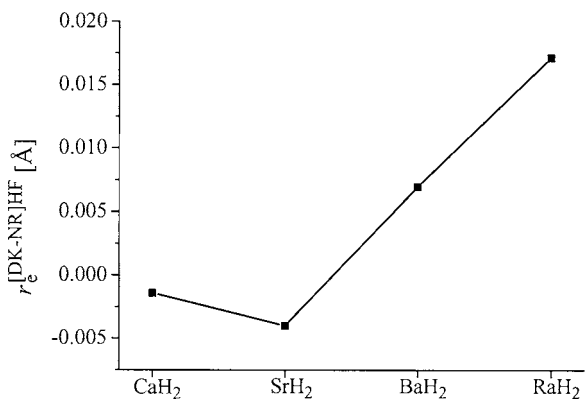

FIG. 2. Relativistic contribution (DK-NR) to the M–H bond lengths, r_e(M–H) from CaH_2 to RaH_2 obtained at the HF level.

Table II compares the equilibrium geometries of this study with previously determined ones. Overall, there is a good agreement for the bond length across the whole spectrum of methods considered. In particular, the $10ve$ pseudopotential results are in excellent agreement with the all-electron results, as shown in Fig. 3. This is encouraging since the small-core definition of the these ECPs successfully in-

TABLE II. Comparison of the equilibrium geometry of the alkaline-earth dihydrides from CaH_2 to RaH_2.

	CaH_2		SrH_2		BaH_2		RaH_2	
Method	r (M–H)	∠ (HMH)	r (M–H)	∠ (HMH)	r (M–H)	∠ (HMH)	r (M–H)	∠ (HMH)
DKCCSD(T)[a]	2.060	180.0	2.184	134.6	2.293	117.3	2.365	111.7
ECP/CCSD(T)[a]	2.060	180.0	2.183	134.9	2.292	117.3	2.372	112.6
ECP/SDCI+Q/f[b]	2.055	180.0	2.201	139.6	2.314	118.7	⋯	⋯
ECP/B3LYP[a]	2.052	180.0	2.165	124.6	2.288	113.6	2.374	109.5
ECP/B3LYP[c]	⋯	⋯	2.164	124.5	2.287	113.1	⋯	⋯

[a]This work.
[b]Quasirelativistic $10\nu e$ ECP including f functions. See Ref. 11.
[c]SDD pseudopotential/B3LYP[6-311++G($3df$,$3pd$)]. See Ref. 22.

corporates, in its explicit valence-only part, the major core-valence correlation contribution and is able to reproduce the bent structure of SrH_2, BaH_2, and RaH_2 without the need for additional core-polarization terms. Although the core-valence treatment in the $10\nu e$ ECP is not complete, the results are quantitative within 1° of all-electron values. As noted by Kaupp *et al.*, it is necessary for the large-core ECP to include not only an extensive d basis but also a core-polarization contribution in order to observe bending in these molecules.[11] The geometries obtained from ECP/DFT calculations with a B3LYP hybrid functional, on the other hand, deviate from AE and ECP/CCSD(T) values, as seen in Table I. Especially notable is the DFT bond angle for SrH_2 showing a discrepancy of up to 10°. The flatness of the potential surface (see later) for SrH_2 may well contribute to the deviation at the DFT level due to its errors in describing dispersion. In fact, for more bent dihydrides DFT results continuously improve and the underestimation of the bond angles is not as profound. It still remains as a general feature of DFT results even at the all-electron DFT level. Further, calculated equilibrium geometries tend to depend on particular functionals chosen. For example, calculated bond distances of SrH_2 are 2.164, 2.154, and 2.130 Å and the bond angle are, 124.6°, 120.6°, and 117.5° at the respective B3LYP, PW91, and LDA levels of theory (Fig. 3). Of these functionals considered, B3LYP functional seems to perform the best. Overall, there is a good agreement among the theoretical equilibrium geometry determined by various authors within the boundary of adopted methods of calculation. The ECP values of Kaupp *et al.*[11] tend to be only slightly larger than the present values, whereas the ECP/DFT values of Wang and Andrews[22] are virtually identical to those of this work. Particularly large deviation of the bond angle for SrH_2 shows the difficulty associated with obtaining accurate geometry for such a floppy molecule with a low barrier height to the linear form.

Linearization energies deserve to be mentioned. They are compiled in Table III. As noted by previous authors, the "genuinely" bent structure starts from BaH_2 and continues to RaH_2. The trend in linearization energy among MH_2 is such that it increases with nuclear charge of the metal and decreases on account of scalar relativity for all. Relativistic effects grow towards heavier metals and become significantly large for RaH_2 with their contribution of up to 29% at

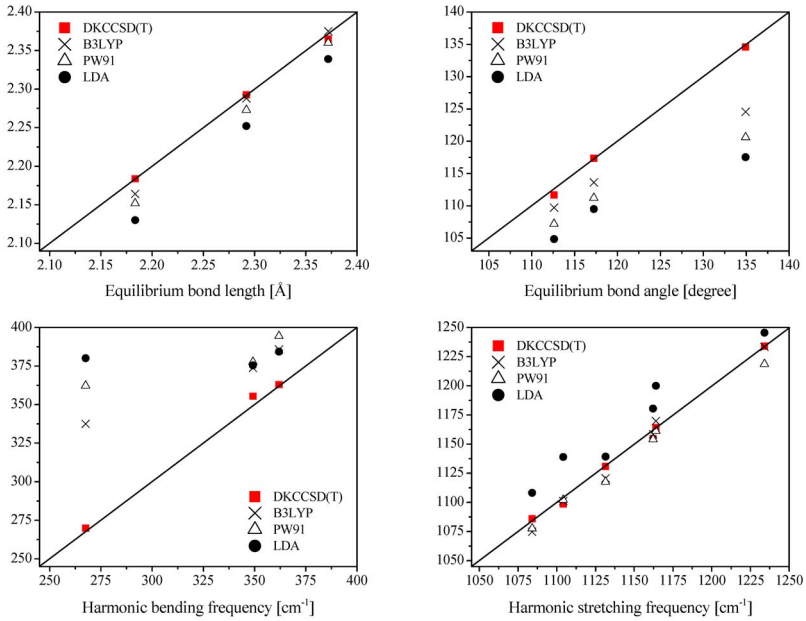

FIG. 3. (Color online) Comparison of calculated values for the alkaline-earth dihydrides from SrH_2 to RaH_2. ECP/CCSD(T) values are plotted on the x axis and other theoretical values on the y axis. DKCCSD(T) values are obtained from all-electron calculations, and DFT values from ECP calculations.

TABLE III. Linearization energy of MH_2 (M=Ca to Ra) obtained at various levels of theory. All values are in kcal/mol.

Method	SrH_2	BaH_2	RaH_2
NRHF	0.61	5.32	7.11
DKHF	0.53	4.40	5.12
NRCCSD(T)	1.49	8.06	9.96
DKCCSD(T)	1.35	6.86	8.01
ECP/CCSD(T)	1.28	7.04	7.72
ECP/DFT	3.29	9.36	9.19
ECP/SDCI+Q/f[a]	0.97	6.06	···

[a]Quasirelativistic $10\nu e$ ECP including f functions. See Ref. 11.

the HF level. The relativistic decrease in the linearization energy is seen to be a destabilizing factor for the bent structures. Other ECP values are considerably underestimated compared with those of this work, whereas the DFT values seem to suffer from overestimation. Moreover, there is a slight decrease in the linearization energy from BaH_2 to RaH_2. Such an irregularity is absent in other calculated properties, especially in the bending force constants, which calls for a further investigation.

The harmonic vibrational frequencies are compiled in Table IV and are compared with literature values in Table V. On a quantitative level, the AE and ECP frequencies determined at the CCSD(T) level are found very close to each other, whereas the ECP/B3LYP values show a considerable deviation from those of wave function based methods (Fig. 3). The upper limit of the discrepancy lies around several tens of wave numbers for the bending frequencies, which is not surprising considering the deviation in the calculated equilibrium bond angles at the ECP/B3LYP level. Qualitatively, however, all values are within agreement among all methods considered. Particularly noteworthy is the general trend observed in the normal modes of vibration. The harmonic frequencies for the symmetric $\nu_s(a_1)$ and antisymmetric $\nu_{as}(b_2)$ stretch modes show a monotonic decrease from CaH_2 to RaH_2. The bending frequency $\nu_b(a_1)$, on the other hand, increases with increasing nuclear charge of the central metal, but this continues only up to BaH_2. For the heavier RaH_2 the bending frequency suddenly drops below that of BaH_2 exhibiting an anomalous trend. Data compiled in Table VI provide more insights into the possible origin of this anomaly through a comparison of force constants k between all-electron nonrelativistic and scalar relativistic DK results. For the sake of clarity we focus on the HF values and note that at the nonrelativistic level the bending force constants are monotonically increasing from CaH_2 to RaH_2. When scalar relativity is taken into consideration the bending force constants become smaller for all metal dihydrides [Fig. 4(a)]. A particularly large relativistic decrease in k_b for RaH_2 causes it to drop from BaH_2 to RaH_2 at the DK level, as shown in Table VI. This indicates that the anomaly in the bending frequency trend is clearly caused by relativity. One may rationalize this nonmonotonous trend in terms of the factors important for bending, core polarization, and d-orbital participation and how they are affected by relativity. Firstly, for the core polarization, the polarized-ion model is considered.[7,19] Using this model one can formulate the bending force constants in terms of the cation and anion dipole polarizabilities and the bond distance between the two. The relationship is such that the smaller the cation dipole polarizabilities and the larger the bond lengths, the smaller the bending force constants. As already pointed out, relativity increases the bond lengths for the heavier metal dihydrides, which lead to smaller bending force constants at the relativistic level in agreement with our observation. As for the cation dipole polarizabilities, the relativistic contributions are increasingly negative from Ca^{2+} to Ra^{2+}, which also supports the changes made to the bending force constants by relativity. Quantitatively, however, an accurate estimation of relativistic effects on the bending frequency is difficult as this model is highly sensitive to the accuracy in cation polarizabilities. Further, the anomalous trend in the bending frequency is not easily predicted. The fact that the covalency of MH_2 is not accounted for and this model is based on a classical interpretation may justify the limitations of this model. As for the d-orbital participation, we consider the population of these orbitals obtained in our all-electron calculations. At the nonrelativistic level the d population is monotonically increasing with increasing nuclear charge of the metal (0.2580, 0.5096, and 0.5162 for SrH_2, BaH_2, and RaH_2, respectively). Upon inclusion of relativity, however, the overall d-orbital participation is reduced for all dihydrides (0.1187, 0.4579, and 0.3944 for SrH_2, BaH_2, and RaH_2, respectively; see also Ref. 20). This decrease in the d-orbital participation translates to a reduced s-d hybridization and hence to a smaller restoring force about bending relative to the nonrelativistic case. Moreover, large relativistic effects associated with RaH_2 leads to a sudden decrease in the d-orbital population from BaH_2 to RaH_2, which gives rise to an anomaly as was observed in the bending force constants at the relativistic level. The decrease in the s-d hybridization due to relativity was previously attributed to a size effect related to the relativistic expansion of d orbital.[20] We suggest, however, that it may be an energy effect related

TABLE IV. Harmonic vibrational frequencies of the alkaline-earth dihydrides, MH_2 (M=Ca to Ra). All values are in cm^{-1}.

	AE/DKCSD(T)			ECP/CCSD(T)			ECP/B3LYP		
	ν_b (a_1)	ν_{as} (b_2)	ν_s (a_1)	ν_b (a_1)	ν_{as} (b_2)	ν_s (a_1)	ν_b (a_1)	ν_{as} (b_2)	ν_s (a_1)
CaH_2	118.1	1251.1	1318.3	123.0	1246.7	1316.3	182.7	1228.3	1320.8
SrH_2	269.9	1164.1	1234.1	267.5	1164.1	1234.1	337.6	1169.9	1233.3
BaH_2	362.9	1098.7	1154.7	361.9	1104.2	1162.1	385.8	1101.2	1158.5
RaH_2	355.5	1086.0	1130.8	349.2	1084.1	1131.5	373.8	1074.8	1120.8

TABLE V. Comparison of the harmonic vibrational frequencies of the alkaline-earth dihydrides, MH_2 (M=Ca to Ra). All values are in cm^{-1}.

	CaH_2			SrH_2			BaH_2		
Method	ν_b (a_1)	ν_{as} (b_2)	ν_s (a_1)	ν_b (a_1)	ν_{as} (b_2)	ν_s (a_1)	ν_b (a_1)	ν_{as} (b_2)	ν_s (a_1)
ECP/HF[a]	155.0	1261.1	1334.3	213.8	1147.5	1237.5	335.8	1066.1	1141.9
ECP/HF[b]	157	1257	1336	213	1148	1237	347	1075	1147
ECP/MP2[c]	⋯	⋯	⋯	233.4	1141.4	1227.6	369.0	1101.3	1171.2
AE/DKCCSD(T)[a]	118.1	1251.1	1318.3	269.9	1164.1	1234.1	362.9	1098.7	1154.7
ECP/CCSD(T)[a]	123.0	1246.7	1316.3	267.5	1164.1	1234.1	361.9	1104.2	1162.1
ECP/B3LYP[a]	⋯	⋯	⋯	337.6	1169.9	1233.3	385.8	1101.2	1158.5
B3LYP[d]	⋯	⋯	⋯	343.6	1159.9	1227.6	389.9	1102.1	1166.6

[a]This work.
[b]Quasirelativistic 10*ve* ECP. See Ref. 11.
[c]6-311++G(3*df*,3*pd*)/SDD pseudopotential. See Ref. 22.
[d]SDD pseudopotential B3LYP[6-311++G(3*df*,3*pd*)]. See Ref. 22.

to the stabilization of the *s* orbital. Indeed, when we consider the two MOs characteristic of *s* and *d* orbitals the respective HOMO-1 and HOMO, we find that the energy separation between these two MOs are increased at the relativistic level where the main contribution is given by the stabilization of the *s* orbital rather than the destabilization of the *d* orbital (Fig. 5). A particularly large stabilization of the HOMO-1 of RaH_2 can easily give rise to the anomaly mentioned above in agreement with the bending force constant trend.

For the stretch modes relativistic effects act to increase the force constants [Fig. 4(b)]. This is peculiar as the usual expectation is such that the larger the bond lengths the smaller the stretching force constants.[21] This is reflected in the overall trend through this series of molecules but does not seem to hold for relativistic effects. Although the relativistic contribution grows larger from Ca to Ra, it is not substantial enough to influence the overall trend.

Experimental vibrational frequencies were found to depend on the matrix environment as a solid matrix may induce cation polarization.[22] This makes it difficult to make a comparison with calculated values. For example, the vibrational frequencies range from 1131.3 to 1128.6 cm^{-1} and from 1100.4 to 1098.0 cm^{-1} for the respective symmetric stretching and antisymmetric stretching modes of vibration depending on the matrix environment.

IV. CONCLUSION

We presented in this paper the ground state equilibrium geometries and vibrational frequencies/force constants of the alkaline-earth dihydrides from CaH_2 to RaH_2. Made available here for the first time are precise harmonic vibrational frequencies determined at the CCSD(T) level as well as a detailed discussion on the role of relativity for these molecules through high level calculations. Relativistic effects in these molecules are not large but become more noticeable especially for the linearization energy and the bending force constants. For the latter particularly large relativistic effects

TABLE VI. Force constants of the alkaline-earth dihydrides, MH_2 (M=Ca to Ra) obtained from all-electron calculations at the nonrelativistic and scalar relativistic levels. All values are in mdyn/Å.

	NR			DK		
	k_b	k_{as}	k_s	k_b	k_{as}	k_s
HF						
CaH_2	0.016	0.988	1.103	0.016	0.990	1.105
SrH_2	0.031	0.784	0.914	0.029	0.793	0.923
BaH_2	0.076	0.658	0.763	0.068	0.681	0.779
RaH_2	0.080	0.592	0.694	0.065	0.656	0.742
MP2						
CaH_2	0.015	0.987	1.089	0.015	0.990	1.091
SrH_2	0.030	0.789	0.903	0.027	0.796	0.911
BaH_2	0.072	0.671	0.759	0.064	0.692	0.775
RaH_2	0.074	0.610	0.693	0.060	0.663	0.735
CCSD(T)						
CaH_2	0.009	0.973	1.082	0.009	0.975	1.083
SrH_2	0.047	0.811	0.913	0.044	0.817	0.919
BaH_2	0.085	0.702	0.787	0.079	0.723	0.799
RaH_2	0.084	0.621	0.705	0.075	0.704	0.763

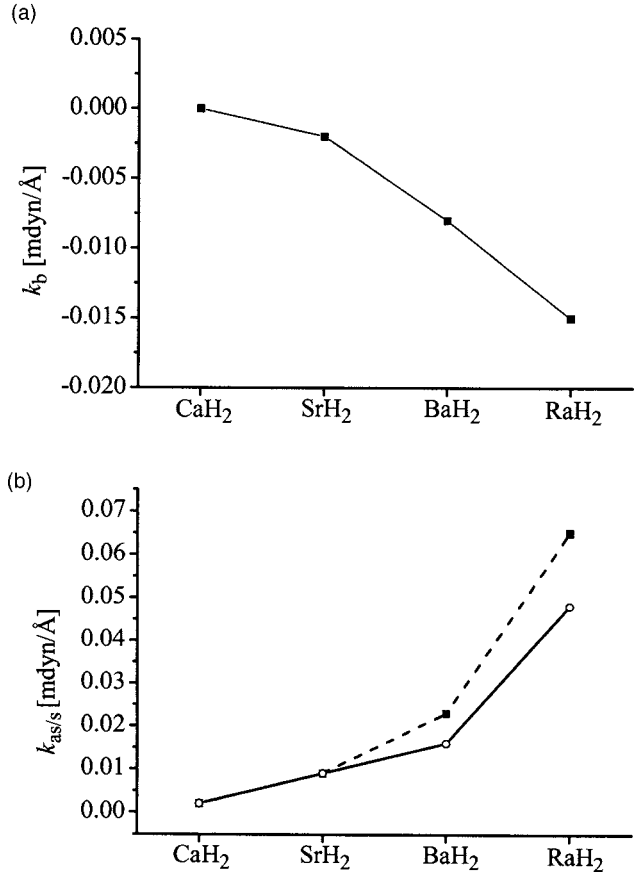

FIG. 4. Relativistic contribution (DK-NR) at the HF level to (a) bending and (b) asymmetric (dashed) and symmetric (solid) force constants k for the alkaline-earth metal dihydrides from CaH_2 to RaH_2.

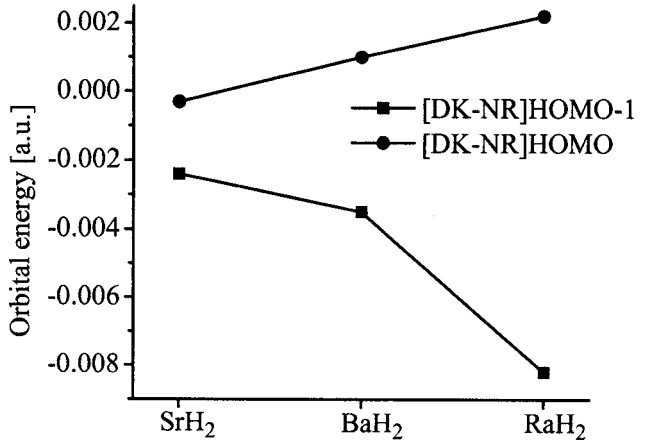

FIG. 5. Relativistic contribution (DK-NR) to the orbital energies of HOMO-1 and HOMO.

give rise to an anomaly in the trend going from BaH_2 to RaH_2. The extent of relativistic effects on these properties is dominated by the relativistic stabilization of the metal *s* orbital, which in turn influences the degree of *s*-*d* hybridization. In this case, there seems to be a straightforward correlation between the level of *d* participation and the bending force constants. Clearly, relativistic effects play an essential role in understanding the observed trend. As for the stretching force constants, no anomalies are observed in the overall trend. Relativistic effects are still present for these modes of vibration, and it will be interesting to investigate the effects on the dihydride of superheavy element 120 where larger relativistic effects are expected.

The performance of recently developed small-core ECP for the alkaline-earth elements is excellent, and the accuracy limit is practically reached compared with all-electron methods. The DFT methods, on the other hand, show large deviations, which is particularly worse for the bond angle and bending frequencies. This suggests that the DFT may not be the best choice of method for floppy molecules such as those studied in this paper.

We note, in conclusion, that the question of bending in alkaline-earth dihydrides or dihalides and the major contributing factors to such a phenomenon have well been investigated previously. It is commonly acknowledged that the *d*-orbital participation and the core polarization play a major role in the structural configuration of these molecules. The fact that both of these factors are highly susceptible to relativistic effects provides opportunities to investigate in detail the contribution of such effects. The use of effective core potentials which implicitly include major relativistic effects is proven successful for such an investigation. For a clear separation of relativistic effects, however, all-electron calculations are still required. The extensiveness of all-electron calculations, especially at the correlated level, may be reduced by the DFT methods provided that reliable results can be obtained. This still remains to be seen. We are currently extending the present work to the case of other AB_2-type triatomic molecules.

ACKNOWLEDGMENTS

This work was supported by the Korea Research Foundation Grant funded by the Korean government (MOEHRD) (KRF-2006-312-C00191) in which computational resources were provided by the supercomputing center of the Korea Institute of Science Technology Information (KISTI) and by a grant (06K1401-01010) from the Center for Nanoscale Mechatronics and Manufacturing, one of the 21st Century Frontier Research Programs, which are supported by the Ministry of Science and Technology, Korea.

[1] M. Kaupp, P. v. R. Schleyer, H. Stoll, and H. Preuss, J. Am. Chem. Soc. **113**, 6012 (1991).
[2] L. Wharton, R. A. Berg, and W. K. Klemperer, J. Chem. Phys. **39**, 2023 (1963).
[3] E. F. Hayes, J. Phys. Chem. **70**, 3740 (1966).
[4] I. Bytheway, R. J. Gillespie, T.-H. Tang, and R. F. W. Bader, Inorg. Chem. **34**, 2407 (1995).
[5] M. Guido and G. Gigli, J. Chem. Phys. **65**, 1397 (1976).
[6] L. v. Szentpály and P. Schwerdtfeger, Chem. Phys. Lett. **170**, 555 (1990).
[7] K. J. Donald, W. H. Mulder, and L. v. Szentpály, J. Chem. Phys. **119**, 5423 (2003).
[8] M. Kaupp, Angew. Chem., Int. Ed. **40**, 3543 (2001).
[9] L. Seijo, Z. Barandiarán, and S. Huzinaga, J. Chem. Phys. **94**, 3762 (1991).
[10] I. S. Lim, H. Stoll, and P. Schwerdtfeger, J. Chem. Phys. **124**, 034107 (2006).
[11] M. Kaupp, P. v. R. Schleyer, H. Stoll, and H. Preuss, J. Chem. Phys. **94**, 1360 (1990).
[12] B. O. Roos, V. Veryazov, and P.-O. Widmark, Theor. Chem. Acc. **111**, 345 (2003).
[13] M. J. Frisch, G. W. Trucks, H. B. Schlegel *et al.*, GAUSSIAN 03, Revision

C.02, Gaussian, Inc., Wallingford, CT, 2004.
[14] H. J. Werner, P. J. Knowles, R. D. Amos *et al.*, MOLPRO, Version 2002.1, a package of *ab initio* programs, Birmingham, UK, 2002.
[15] G. Karlström, R. Lindh, P.-Å. Malmqvist *et al.*, Comput. Mater. Sci. **28**, 222 (2003).
[16] T. A. Albright, J. K. Burdett, and M. Whangbo, *Orbital Interactions in Chemistry* (Wiley, New York, 1985).
[17] T. Ziegler, J. G. Snijders, and E. J. Baerends, Chem. Phys. Lett. **75**, 1 (1980); J. Chem. Phys. **74**, 1271 (1981); P. Pyykkö, J. G. Snijders, and E. J. Baerends, Chem. Phys. Lett. **83**, 432 (1981).
[18] I. S. Lim and P. Schwerdtfeger, Phys. Rev. A **70**, 062501 (2004).
[19] R. L. Dekock, M. A. Peterson, L. K. Timmer, E. J. Baerends, and P. Vernooijs, Polyhedron **9**, 1919 (1990); **10**, 1965(E) (1991).
[20] P. Pyykkö, J. Chem. Soc., Faraday Trans. 2 **75**, 1265 (1979).
[21] B. I. Baikov, Opt. Spektrosk. **27**, 923 (1969).
[22] X. Wang and L. Andrews, J. Phys. Chem. A **108**, 11500 (2004).